Supporting information

Uncorrelated Effect of Interdomain Contact on Pin1 Isomerase Activity Reveals Positive Catalytic Cooperativity

Wenkai Zhu[†,‡], *Ying Li*[†], *Maili Liu*[†,‡,*], *Jiang Zhu*[†,*], *Yunhuang Yang*[†]

† State Key Laboratory of Magnetic Resonance and Atomic Molecular Physics, Key Laboratory of Magnetic Resonance in Biological Systems, National Center for Magnetic Resonance in Wuhan, Wuhan Institute of Physics and Mathematics, Chinese Academy of Sciences, Wuhan 430071, P.R. China
‡ University of Chinese Academy of Sciences, Beijing 100049, P.R. China

AUTHOR INFORMATION
Corresponding Author
* jiangzhu@wipm.ac.cn
* ml.liu@wipm.ac.cn

Experimental Methods

Expression and purification of Pin1 and its variants

For expressing full length version (M1-E163) and isolated PPIase domain (G45-E163) of human Pin1, the encoding DNA fragments were cloned into a pET32m expression vector[1] including a N-terminal 6×His tag, respectively. For expressing isolated WW domain (M1-G39) of human Pin1, the corresponding DNA fragment was cloned into a pGEX4T expression vector including a glutathione S-transferase (GST) tag at the N-terminal. The recombinant plasmids were transformed into *Escherichia coli* BL21 (DE3) for protein expression. The *E. coli* cells harboring the recombinant plasmid were grown in LB or M9 minimal medium at 37 °C until OD_{600} reached 0.6, and subsequently 0.5 mM isopropyl-β-D-thiogalactopyranoside (IPTG) was added to induce protein expression overnight at 24 °C. The cells were harvested and lysed by sonication, and supernatant was clarified through centrifugation and filtration and then subjected to purification using an ÄKTAxpress™ (GE Healthcare) equipped with a Ni-affinity column (HisTrap IMAC HP™ column, 5 mL) or a GST-affinity column (GSTrap™ HP, 5 mL). The 6×His tag or GST tag was further removed from the target protein through thrombin digestion at 4 °C overnight. Finally, the target protein was purified using a gel filtration column (HiLoad 26/60 Superdex 75) and concentrated into the NMR buffer (50 mM Tris, 5 mM DTT, 0.3% NaN_3, pH 6.8). The plasmids for expressing the site-specific mutants of Pin1 such as $Pin1_{L86C}$, $Pin1_{I28A}$, $Pin1_{W34A}$ and $Pin1_{W34A/R17A}$, as well as the linker-modified mutants of Pin1 such as $Pin1_{G5}$, $Pin1_{del}$, $Pin1_{\Delta SG}$, $Pin1_{\Delta NSSSG}$ and $Pin1_{\Delta NSSSGNG}$, were obtained using a polymerase chain reaction (PCR)-based mutagenesis method, and following expression and purification of the desired mutant protein were carried out using a similar method to that for wild-type full length Pin1. $^{15}NH_4Cl$ and ^{13}C-glucose were used in M9 minimal medium for isotope labeling.

Preparation of Pin1 substrate peptides

The substrate peptides of Pin1, including EQPLpTPVTDL (pCdc25C), FFpSPR, and maleimide-terminated KSPTpSPS, were synthesized by GL Biochem Ltd. (Shanghai). The purities of the peptides were determined to be above 98% through high performance liquid chromatography (HPLC) analysis, and their molecular weights were confirmed through electrospray ionization mass spectrometry (ESI-MS).

Chemical shift assignment

3D HNCACB and CBCA(CO)NH and 2D ^{1}H-^{15}N HSQC spectra of Pin1 were collected at 298 K on a Bruker Avance III 850 MHz spectrometer for chemical shift assignment. Backbone resonances for 144 out of 156 non-proline amide residues were assigned, except those for M1 and R17-S19 in the WW domain, S38, N40-S43, N47 and G48 in interdomain linker, and E76 in the PPIase domain. The backbone assignments of Pin1 were transferred to PPIase domain (G45-E163) with the aid of previously published assignments of the PPIase domain (BMRB accession code: 11559). The chemical shifts for substrate peptides were assigned by homonuclear TOCSY and NOESY spectra.

Sample preparation of the $Pin1_{L86C\text{-}substrate}$

The residue L86 in α1 helix of Pin1 PPIase domain (Figure S6) was mutated to cysteine for conjugation with the maleimide-terminated substrate peptide (KSPTpSPS), considering the merits

of L86 that it is solvent exposed, distant from the interdomain interface and close to the interdomain concave (Figure 2B). After expression and purification, $Pin1_{L86C}$ was exchanged into a reaction buffer containing 10 mM Tris (pH 7.6) and subsequently mixed with the substrate peptide in the same buffer at a ratio of 1:1. The conjugation reaction was allowed to proceed for 1 h at 4 °C, and the completion of the reaction was checked through mass spectrometry. There are two innate cysteines, C57 and C113 in Pin1 that may react with the maleimide-terminated peptide. Thus, the correct construction of $Pin1_{L86C\text{-}substrate}$ was confirmed through mass spectrometry and NMR spectroscopy. Only the product with single-conjugated peptide was observed in mass spectrometry analysis (Figure S4), and ^{1}H-^{15}N HSQC spectrum comparison of Pin1 and the $Pin1_{L86C\text{-}substrate}$ showed that the cross-peaks of C57 and C113 were not affected by the conjugation reaction (Figure S5). Besides, if other low-populated single conjugation products exist, there will be two sets of cross-peaks for interdomain interfacial residues such as A140, L141, G128 and G148, which were not found in the HSQC spectrum.

NMR spin relaxation experiment and analysis

Backbone ^{15}N R_1 and R_2 relaxation rates and steady-state ^{15}N heteronuclear NOE (hNOE) values of Pin1 were measured on a Bruker 600MHz spectrometer at 298 K, and backbone ^{15}N R_1 and R_2 relaxation rates of $Pin1_{L86C\text{-}substrate}$ were measured on a Bruker 700MHz spectrometer at 298 K, each equipped with a cryogenic probe. All spectra were recorded with 256×1024 complex points. All data were processed using NMRPipe.[2] The ^{15}N R_1 and R_2 relaxation rates were determined by fitting peak heights as a function of relaxation delay times using "rh" function in SPARKY,[3] and the uncertainties were estimated by Monte Carlo analysis based on the spectrum noise. The delays for R_1 measurements were 0.01, 0.12, 0.30, 0.50, 0.70, 1.00, and 2.00 s, and for R_2 measurements were 16.96, 50.88, 84.80, 101.76, 135.68, 169.60, and 203.52 ms. The spectra for R_1 and R_2 were recorded in an interleaved manner with a recycle delay of 2.00 s. For the steady-state ^{15}N hNOE experiment, the spectra were recorded in an interleaved manner with or without proton saturation in a recycle delay of 8.00 s. Steady-state hNOE values were derived from the ratios between the peak intensities with and without proton saturation.

Residual Dipolar couplings (RDCs) measurement and analysis

The RDCs ($^{1}D_{NH}$) were derived by taking the differences in J_{NH} on an aligned ($C_{12}E_5$/hexanol) and an isotropic (buffer) sample using the ARTSY-HSQC experiment[4] at 600 MHz or 700 MHz. The alignment of samples was achieved by adding 16% (v/v) PEG stock into the protein samples yielding a final medium concentration of 4.5% (v/v) with a protein concentration of 0.3 mM. The alignment tensor and predicted RDCs were obtained using a singular value decomposition (SVD) program in NMRPipe, based on the structure coordinates of the crystal structure (PDB ID: 1PIN) and the experimental RDC values for the individual domain of Pin1, separately (Table S1).

Small angle X-ray scattering (SAXS) data collection and analysis

SAXS data were collected in Shanghai Synchrotron Radiation Facility, at the BL19U2 BioSAXS beamline with a wavelength of 1.240 Å and a sample-to-detector distance of 1.0 m. The range of momentum transfer covered was $0.007 < q < 0.430$ Å^{-1} ($q = 4\pi \sin\theta/\lambda$, where 2θ is the scattering angle, λ is the wavelength). The data for Pin1 and $Pin1_{I28A}$ were collected at two different concentrations (2 mg/ml and 5 mg/ml) and analyzed using program PRIMUS from the ASTAS package.[5] No concentration-dependent effect was found after comparing the two I(q) curves of

different concentrations. Data collected at high concentration (5 mg/ml) were used for further analysis. The data for $Pin1_{L86C\text{-}substrate}$ were collected at a concentration of 1 mg/ml. The theoretical I(q) scattering curves for the crystal structure (PDB ID: 1PIN) and the NMR structure (PDB ID: 1NMV) were calculated using CRYSOL,[6] and subjected to indirect Fourier transformation for obtaining particle distance distribution function P(r) using GNOM.[7] The missing loops in the crystal structure 1PIN were added and refined by MODLLER.[8] The maximum dimension (D_{max}) of the scattering particle was obtained from P(r) by GNOM. The experimental scattering curves of Pin1, $Pin1_{I28A}$ and $Pin1_{L86C\text{-}substrate}$ were normalized by the first point of the experimental scattering data I(0), prior to the linear combination for fitting the experimental curve of Pin1. Ensemble optimization method (EOM)[9] was used to generate an ensemble of various conformations (Figure S2) for evaluating the interdomain flexibility of Pin1. The interdomain linker (R36-R54) and N-terminal residues (M1-L7) showing heteronuclear NOE below 0.65 (data not shown) were allowed to be flexible, while the region V55-E163 in the PPIase domain and the region P8-E35 in the WW domain were treated as rigid bodies. The PPIase domain was fixed, while the WW domain was allowed to be flexible during EOM analysis.

Chemical shift correlation analysis

All data were collected on the Bruker Avance III 850 MHz spectrometer at 298 K. The ^{1}H-^{15}N HSQC spectra of Pin1 and the PPIase domain were overlaid to identify residues affected by interdomain contact (Figure S6). The residues showing chemical shift perturbation value < 0.021 ppm were firstly precluded for chemical shift correlation analysis. Subsequently, the spectrum of $Pin1_{L86C\text{-}substrate}$ was included, and the residues that showed severely overlapped cross-peaks in the overlaid three spectra were also discarded. Finally, ^{15}N and ^{1}H chemical shifts of the retained residues were extracted separately and fitted globally to gauge the population of the compact state using the equation (1),

$$\delta_{Pin1} = p_a \times \delta_{compact} + (1 - p_a) \times \delta_{extended} \quad (1)$$

The chemical shift perturbation ($\Delta\delta$) between the spectra of Pin1 and the PPIase domain were calculated using the equation (2),

$$\Delta\delta = \sqrt{\Delta\delta_H{}^2 + (0.154 \times \Delta\delta_N)^2} \quad (2)$$

Isomerization rate measurement and analysis

The ^{1}H-^{1}H exchange spectroscopy (EXSY) experiments were performed on a Bruker 700 MHz spectrometer at 295 K in Tris buffer (pH 6.8) with 50 μM Pin1 and 2 mM substrate peptide to measure the isomerization rate. Experimental temperature (295 K) was kept same as that reported by other groups previously for data cross-validation.[10-11] The mixing times were 5, 10, 15, 25, 35, 50, 75, 100, and 200 ms. The respective *trans*-to-*cis* and *cis*-to-*trans* isomerization rate were extracted to fit the equation (3) that quantifies the change of the I_{tc}/I_{tt} values with mixing times. The cross-peaks of pT5HN and pS3HN from pCdc25C and FFpSPR, respectively, were used for fitting to the two-state expression as below,

$$\frac{I_{tc}}{I_{tt}}(t_m) = \frac{(1-e^{-(k_{tc}+k_{ct})\times t_m})\times k_{tc}}{k_{ct}+k_{tc}\times e^{-(k_{tc}+k_{ct})\times t_m}} \qquad (3)$$

The measured isomerization rate is related to reversible Michaelis–Menten equation[12] as below,

$$k_{EXSY} = k_{tc} + k_{ct} = \left(\frac{k_{cat}^{trans}}{K_{M,trans}} + \frac{k_{cat}^{cis}}{K_{M,cis}}\right)\frac{E_T}{1+\frac{[trans]}{K_{M,trans}}+\frac{[cis]}{K_{M,cis}}} \qquad (4)$$

The k_{tc} and k_{ct} correspond to the *trans*-to-*cis* and the *cis*-to-*trans* isomerization rate, respectively. E_T is the total enzyme concentration, K_M is Michaelis constant, and the [trans] and [cis] are the *trans* and *cis* substrate concentration, respectively.

NMR titration

NMR titrations of Pin1 with FFpSPR and pCdc25C were performed on the Bruker Avance III 700 MHz instrument at 298 K. The spectra were processed by NMRPipe and further analyzed by SPARKY. The substrate peptides were dissolved in the NMR buffer to a concentration of 20 mM with pH adjusted to 6.8 before titrated into 0.2 mM Pin1 solution. The ^{1}H-^{15}N HSQC spectra of Pin1 mixed with different concentrations of substrate peptide were recorded respectively. To determine the dissociation constant (K_d), chemical shift perturbations ($\Delta\delta$) were extracted and fitted to a two-state binding equation as below,

$$\Delta\delta = \frac{\Delta\delta_{max}}{2}\left\{\left(1+\frac{L_T}{P_T}+\frac{K_d}{P_T}\right) - \sqrt{\left(1+\frac{L_T}{P_T}+\frac{K_d}{P_T}\right)^2 - 4\times\frac{L_T}{P_T}}\right\} \qquad (5)$$

The $\Delta\delta$ at each titration point was calculated using equation (2). $\Delta\delta_{max}$ was defined as the maximum chemical shift perturbation at the saturation point (Pin1:substrate = 1:4) and was adjustable as well as K_d. P_T was fixed to 0.2 mM during the titration and L_T was the concentration of total substrate titrated into the protein sample.

Prediction of the affinity of Pin1$_{\Delta NSSSG}$ for FFpSPR

Besides the K_d fitted from the NMR titration data, the affinity of Pin1$_{\Delta NSSSG}$ for FFpSPR could also be calculated from binding polynomials[13], which correlates with state-specific associate constants and state populations as described in an allosteric cycle (Figure S11A). Since populations of compact state have already been determined for both Pin1 and Pin1$_{\Delta NSSSG}$, the isolated WW domain could be considered as the extended state without compact state, and the K_d (K_a^{-1}) values of the compact state and the extended state could be calculated based on the K_d values of Pin1 and the isolated WW domain, thus the K_d value of Pin1$_{\Delta NSSSG}$ for FFpSPR could be calculated to be 145 μM using equation (6), which agrees well with the value of 139 μM fitted from the NMR titration data.

$$K_{a,obs} = p_a \times K_{a,compact} + (1 - p_a) \times K_{a,extended} \qquad (6)$$

References

(1) Li, T.; Li, S.; Liang, C.; Zhu, J.; Liu, M.; Yang, Y. Chemical shift assignments of RHE_RS02845, a NTF2-like domain-containing protein from Rhizobium etli. *Biomol. NMR. Assign.* **2018**, *12*, 249-252.

(2) Delaglio, F.; Grzesiek, S.; Vuister, G. W.; Zhu, G.; Pfeifer, J.; Bax, A. NMRPipe: a multidimensional spectral processing system based on UNIX pipes. *J. Biomol. NMR.* **1995**, *6*, 277-293.

(3) Lee, W.; Tonelli, M.; Markley, J. L. NMRFAM-SPARKY: enhanced software for biomolecular NMR spectroscopy. *Bioinformatics.* **2015**, *31*, 1325-1327.

(4) Fitzkee, N. C.; Bax, A. Facile measurement of ^{1}H-^{15}N residual dipolar couplings in larger perdeuterated proteins. *J. Biomol. NMR.* **2010**, *48*, 65-70.

(5) Konarev, P. V.; Volkov, V. V.; Sokolova, A. V.; Koch, M. H. J.; Svergun, D. I. PRIMUS: a Windows PC-based system for small-angle scattering data analysis. *J. Appl. Cryst.* **2003**, *36*, 1277-1282.

(6) Svergun, D.; Barberato, C.; Koch, M. H. J. CRYSOL - A program to evaluate x-ray solution scattering of biological macromolecules from atomic coordinates. *J. Appl. Cryst.* **1995**, *28*, 768-773.

(7) Semenyuk, A. V.; Svergun, D. I. Gnom - a program package for small-angle scattering data-processing. *J. Appl. Cryst.* **1991**, *24*, 537-540.

(8) Fiser, A.; Sali, A. MODELLER: Generation and refinement of homology-based protein structure models. *Methods. Enzymol.* **2003**, *374*, 461-491.

(9) Tria, G.; Mertens, H. D. T.; Kachala, M.; Svergun, D. I. Advanced ensemble modelling of flexible macromolecules using X-ray solution scattering. *IUCrJ.* **2015**, *2*, 207-217.

(10) Wang, X.; Mahoney, B. J.; Zhang, M.; Zintsmaster, J. S.; Peng, J. W. Negative regulation of peptidyl-prolyl isomerase activity by interdomain contact in human Pin1. *Structure*. **2015**, *23*, 2224-2233.

(11) Wilson, K. A.; Bouchard, J. J.; Peng, J. W. Interdomain interactions support interdomain communication in human Pin1. *Biochemistry*. **2013**, *52*, 6968-6981.

(12) Greenwood, A. I.; Rogals, M. J.; De, S.; Lu, K. P.; Kovrigin, E. L.; Nicholson, L. K. Complete determination of the Pin1 catalytic domain thermodynamic cycle by NMR lineshape analysis. *J. Biomol. NMR.* **2011**, *51*, 21-34.

(13) Moleschi, K. J.; Akimoto, M.; Melacini, G. Measurement of state-specific association constants in allosteric sensors through molecular stapling and NMR. *J. Am. Chem. Soc.* **2015**, *137*, 10777-10785.

Table S1. Da values for individual domain of Pin1 and $Pin1_{L86C\text{-}substrate}$.

Variant	Da value		Q factor	
	WW	PPIase	WW	PPIase
Pin1	5.2	13.4	37.7%	22.5%
$Pin1_{L86C\text{-}substrate}$	9.8	11.3	35.6%	28.1%

Table S2. Fitting of combined experimental scattering curves of $Pin1_{I28A}$ and $Pin1_{L86C\text{-}substrate}$ at different ratios to that of Pin1.

$Pin1_{L86C\text{-}substrate}$ ratio	0	10%	22%	40%	50%
χ^2	3.06	1.25	1.09	2.50	3.66
Adjusted p value	0.00	0.00	0.03	0.00	0.00

Table S3. Chemical shifts and ($\delta_{compact}$ -δ_{PPIase}) values of the interfacial residues that are used in chemical shift correlation analysis

Residue	PPIase		$Pin1_{L86C\text{-}substrate}$		$\delta_{compact}$ -δ_{PPIase} (ppm)[a]	
	^{1}H (ppm)	^{15}N (ppm)	^{1}H (ppm)	^{15}N (ppm)	^{1}H (ppm)	^{15}N (ppm)
G128[b]	10.231	112.700	10.100	112.262	0.131	0.438
F134	6.902	116.386	6.775	115.555	0.127	0.831
E135	8.637	123.007	8.752	123.199	0.115	0.192
D136	9.101	118.867	9.130	118.310	0.029	0.557
A137	7.027	118.984	6.983	118.193	0.044	0.791
S138	7.814	113.785	7.777	112.667	0.037	1.118
F139	8.171	115.139	7.837	112.881	0.334	2.258
A140	6.877	118.906	7.206	120.810	0.329	1.904
L141	6.836	120.044	6.907	121.903	0.071	1.859
S147	9.617	123.606	9.560	122.619	0.057	0.987
G148	7.692	103.147	7.554	103.418	0.138	0.271
I158[b]	8.426	115.769	8.521	116.572	0.095	0.803

[a] ($\delta_{compact}$ -δ_{PPIase}) values of the interfacial residues provide a "conformational ruler" to quantify the extent of interdomain contact of Pin1 and its variants, which could be used for dynamic and functional studies in future by other groups as long as the ^{1}H-^{15}N HSQC spectrum of Pin1 is recorded under similar experimental conditions. Although chemical shifts are sensitive to local environment (*e.g.* buffer) and referencing, ($\delta_{compact}$ -δ_{PPIase}) and ($\delta_{variant}$ -δ_{PPIase}) values are less sensitive. The population of compact state (p_a) for the Pin1 variant can be calculated using an equation as below,

$$p_a = \frac{\delta_{variant} - \delta_{PPIase}}{\delta_{compact} - \delta_{PPIase}}$$

Since ($\delta_{compact}$ -δ_{PPIase}) values remain constant and are provided in this study, only ($\delta_{variant}$ -δ_{PPIase}) values are needed to gauge state populations of Pin1 variants.

[b] Residues G128 and I158 are not involved in interdomain interface but are sensitive to interdomain contact change due to allosteric effects mediated by hydrogen bond networks formed with interfacial residues.

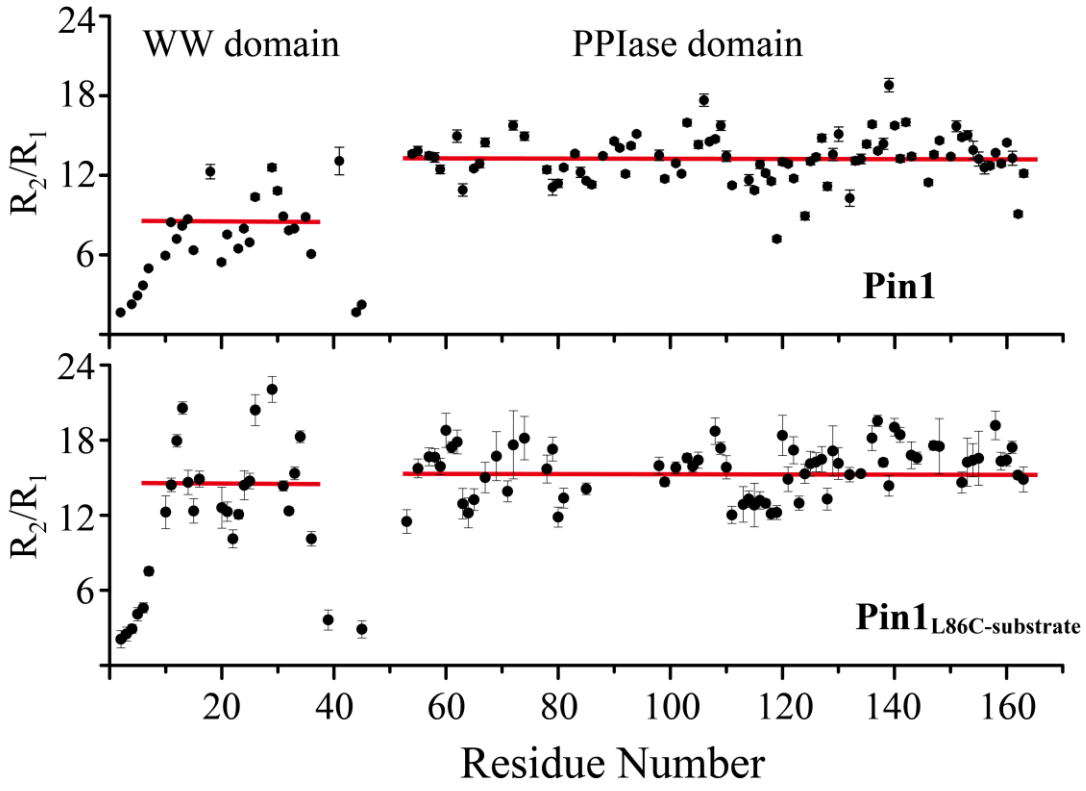

Figure S1. NMR spin relaxation study of Pin1 and $Pin1_{L86C\text{-}substrate}$. ^{15}N R_1 and R_2 values were measured for Pin1 and $Pin1_{L86C\text{-}substrate}$, respectively. The average values of R_2/R_1 for individual domain are extracted from residues in secondary structure elements and depicted by red line. The significant difference between the average R_2/R_1 ratios for the WW domain and the PPIase domain of Pin1 suggests that the two domains tumble independently to a significant extent, whereas the comparable average R_2/R_1 ratios for the two domains of $Pin1_{L86C\text{-}substrate}$ suggest that the two domains tumble as a single entity.

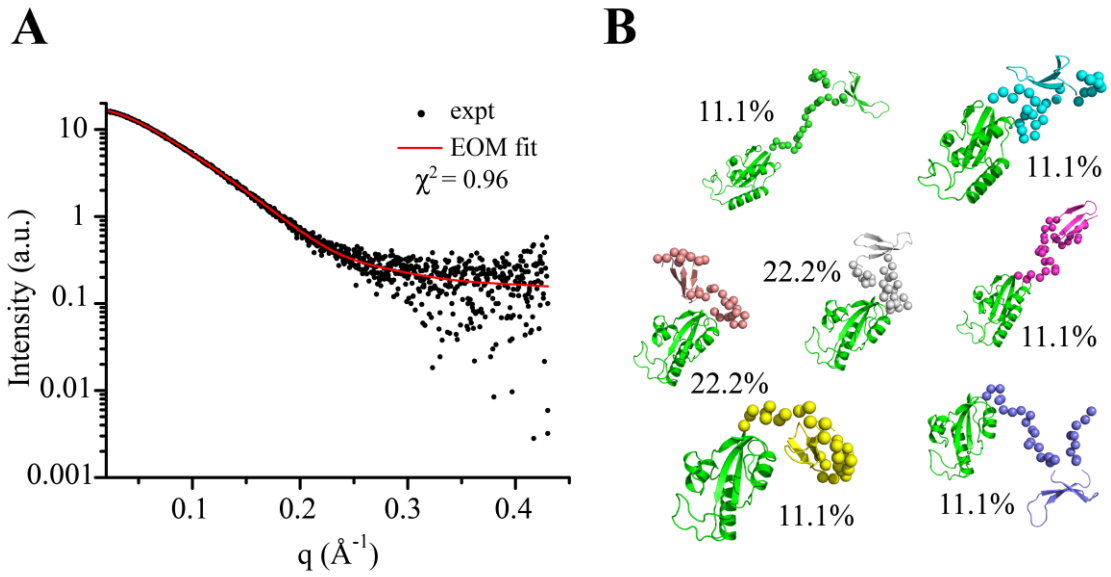

Figure S2. EOM analysis of Pin1. (A) Fitting of the theoretical scattering curve (red curve) from the selected ensemble of 7 models shown in (B) to the experimental scattering data of Pin1 (black dots) with a χ^2 value of 0.96. (B) The selected 7 models from EOM analysis and their respective populations. The interdomain linker (R36-R54) and N-terminal seven residues (M1-L7) were allowed to be flexible during EOM analysis and are depicted in spheres.

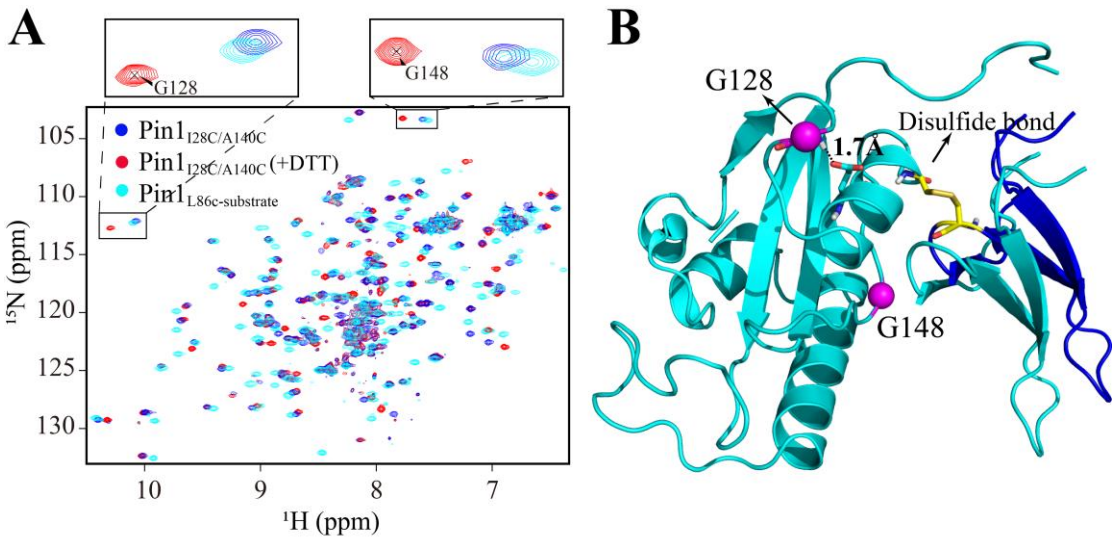

Figure S3. Stabilization of the compact state of Pin1 by disulfide trapping. Two residues I28 and A140 that are close in space according to the crystal structure 1PIN were mutated to cysteines to trap the compact state of Pin1 through disulfide cross-linking. (A) Overlaid ^{1}H-^{15}N HSQC spectra of $Pin1_{L86C\text{-}substrate}$ (cyan) and $Pin1_{I28C/A140C}$ with (red) and without DTT (blue). The cross-peaks of G128 and G148 are zoomed for clarity. (B) The structural model of the compact state of Pin1 obtained through I28C and A140C-mediated disulfide trapping. The expected disulfide bond formed between I28C and A140C is shown as sticks. The positions of G128 and G148 are emphasized by magenta spheres. The spectrum of $Pin1_{I28C/A140C}$ is DTT dependent, indicating the formation of the intramolecular disulfide bond. However, most interfacial residues are suffered from mutational effects caused by I28C and A140C substitution and therefore not suitable for chemical shifts analysis. Moreover, upon adding DTT, the cross-peaks of Gly128 and Gly148 in $Pin1_{I28C/A140C}$ shift towards a compact conformation, but the peak positions of Gly128 suggest a more compact conformation of $Pin1_{I28C/A140C}$ than $Pin1_{L86C\text{-}substarte}$, while the peak positions of Gly148 suggest a less compact conformation of $Pin1_{I28C/A140C}$ than $Pin1_{L86C\text{-}substarte}$. Thus, the state populations calculated from the two residues would be significantly different. It is speculated that, due to disulfide cross-linking, the entire WW domain is likely pulled upwards as shown in (B) by blue color, which could be referred to a “structural distortion”.

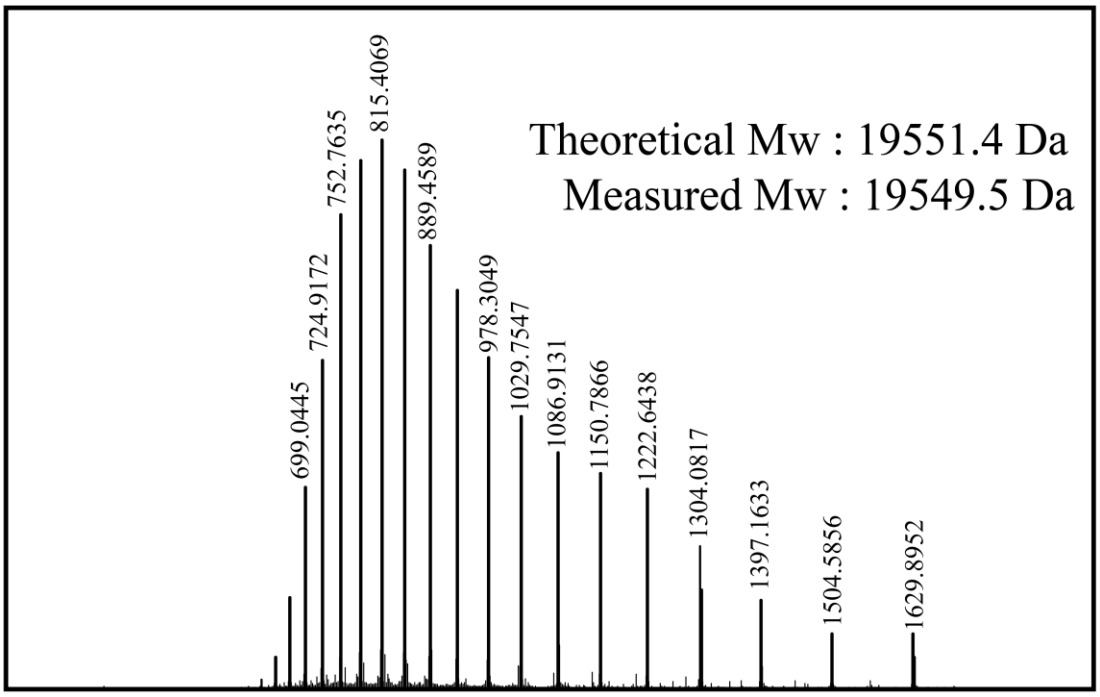

Figure S4. Mass spectrometry analysis of $Pin1_{L86C\text{-}substrate}$. ESI-MS was used to confirm the conjugation of the maleimide-terminated substrate peptide to $Pin1_{L86C}$. The obtained $Pin1_{L86C\text{-}substrate}$ shows an increase of 932.8 Da in molecular weight (MW), equal to the MW of the substrate peptide, evidencing the formation of single conjugation product.

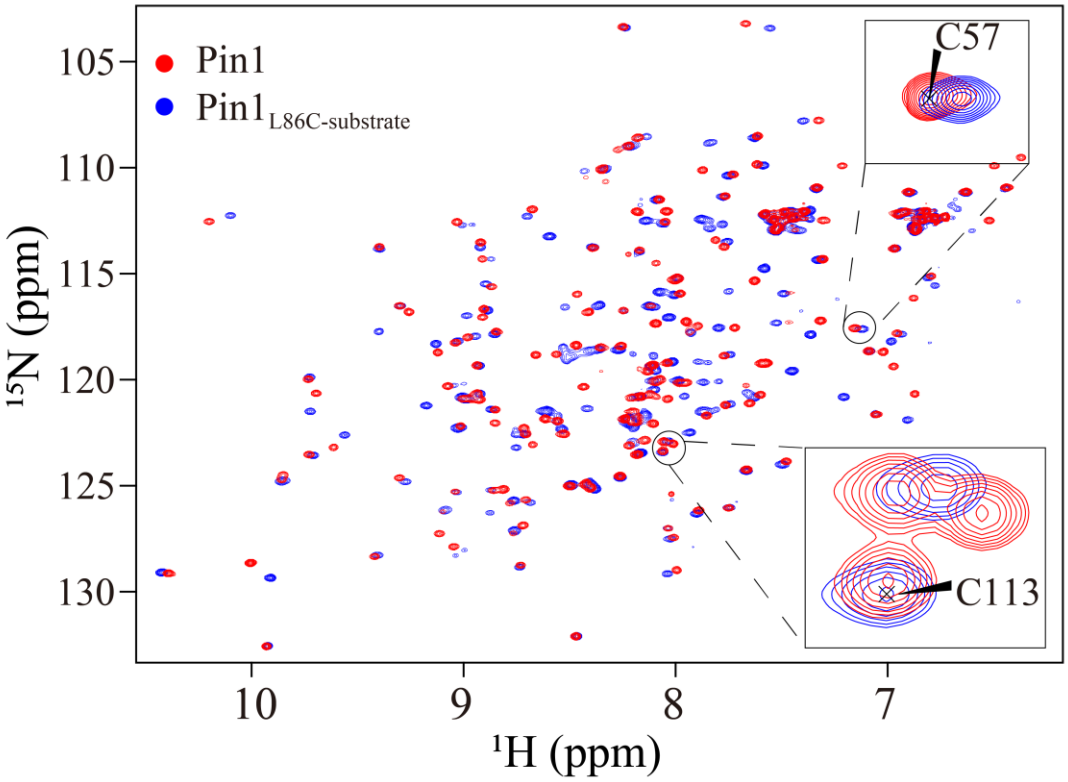

Figure S5. Overlaid ^{1}H-^{15}N HSQC spectra of Pin1 (red) and Pin1$_{L86C\text{-}substrate}$ (blue). The covalent linkage of the substrate peptide to C86 gives rise to widespread chemical shift perturbations in both the WW and PPIase domain of Pin1$_{L86C}$, implying the binding of the WW domain with the substrate peptide and the formation of a compact state. The cross-peaks of C57 and C113 are zoomed as insets to show that they are not affected by L86C mutation and substrate peptide conjugation, which therefore suggests that the substrate peptide exclusively reacts with solvent-exposed C86 under the conditions.

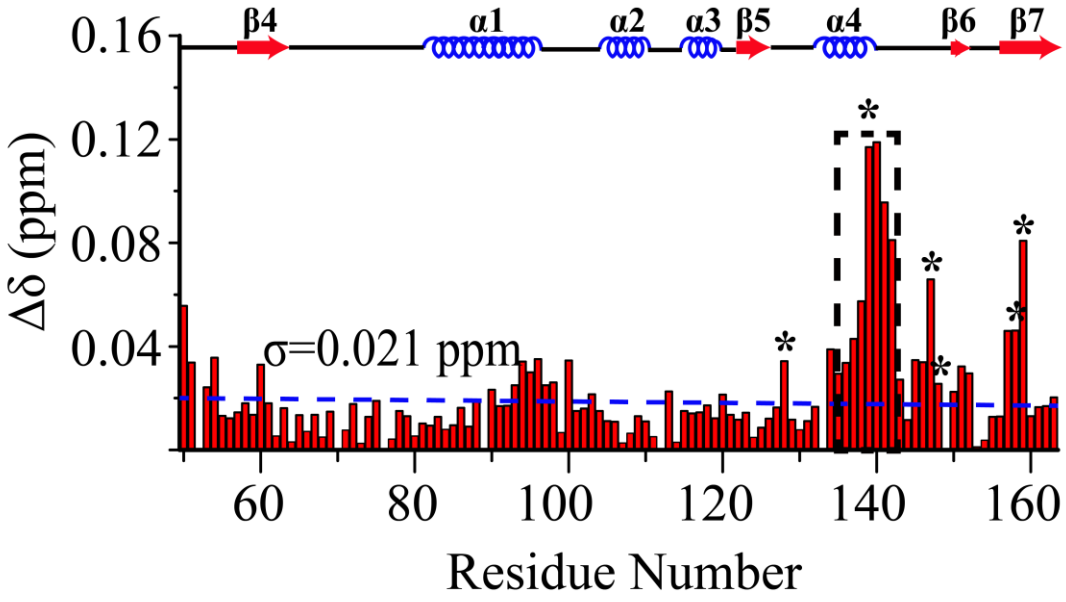

Figure S6. Chemical shift perturbations (Δδ) of Pin1 due to deletion of the WW domain. The Δδ values were calculated based on the ^{1}H-^{15}N HSQC spectra of Pin1 and isolated PPIase domain (G45-E163). The resulted Δδ values were plotted versus residue number to identify residues involved in interdomain contact. The residues labeled by asterisks with Δδ larger than standard deviation (σ) were selected to report on two-state dynamic equilibrium and used in chemical shift correlation analysis to gauge state populations. Secondary structural elements of the PPIase domain were shown on top, and the residues in interdomain interface are highlighted with dashed box.

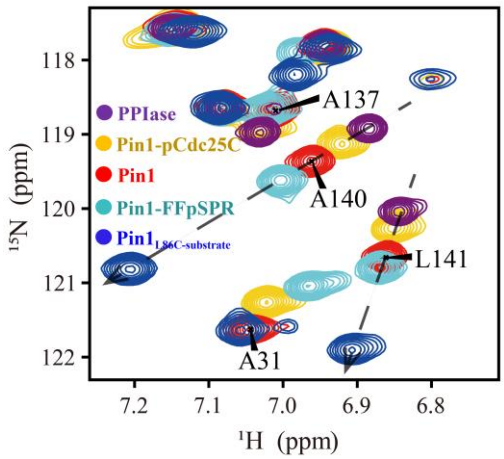

Figure S7. Substrate binding changes the extent of interdomain contact of Pin1. The ^{1}H-^{15}N HSQC spectra of the isolated PPIase domain, Pin1$_{L86C\text{-}substrate}$, apo Pin1, FFpSPR-bound Pin1, and pCdc25C-bound Pin1 were overlaid and partially shown. The cross-peaks of A140 and L141 move downfield towards those of Pin1$_{L86C\text{-}substrate}$ upon FFpSPR binding, whereas move upfield towards those of the isolated PPIase domain upon pCdc25C binding, suggesting an enhanced or a weakened interdomain contact, respectively.

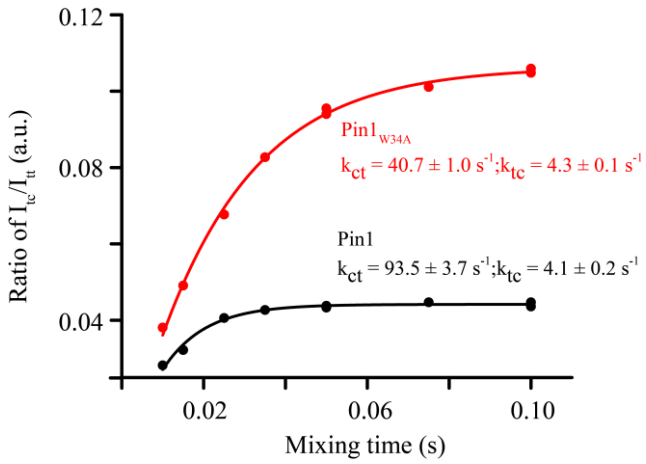

Figure S8. The isomerization rates of Pin1 (black) and $Pin1_{W34A}$ (red) for FFpSPR were determined using ^{1}H-^{1}H EXSY experiments.

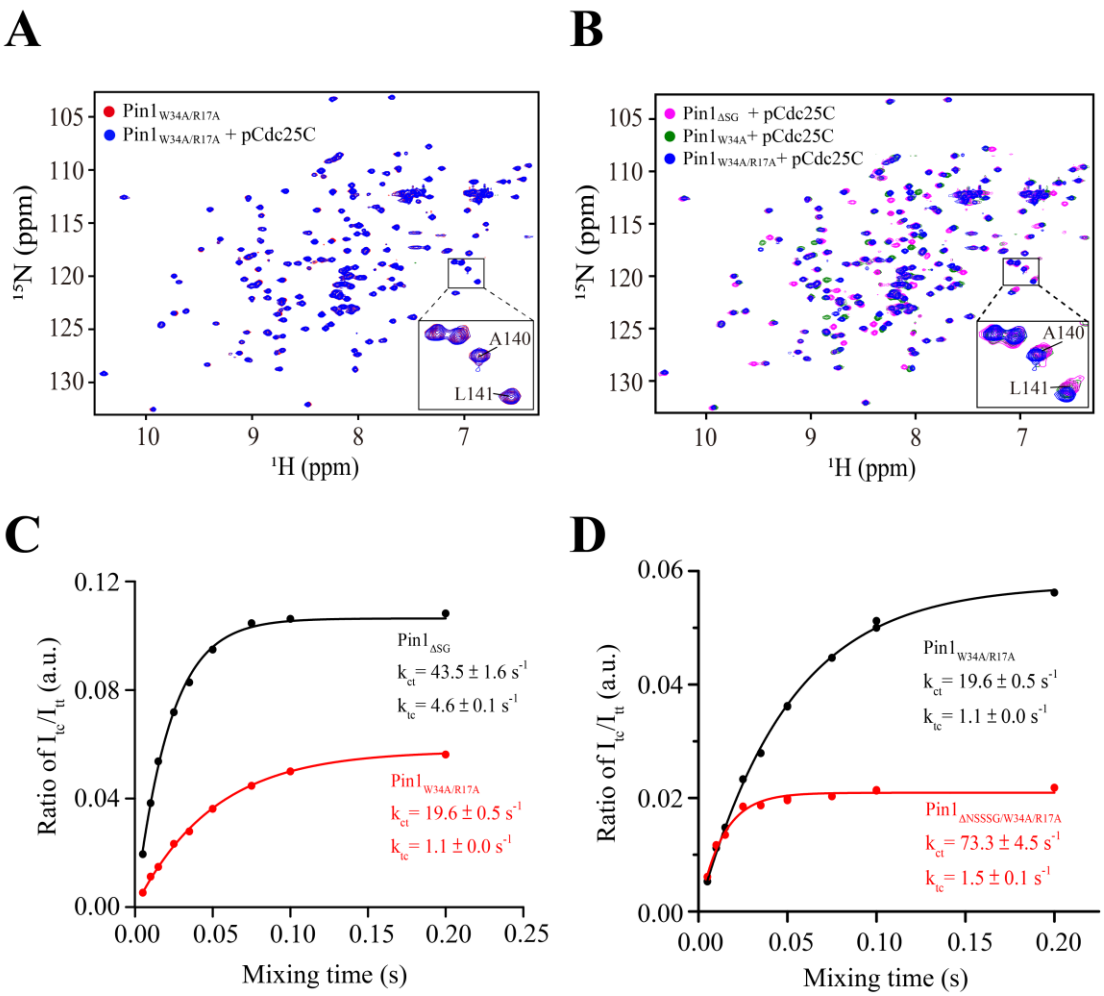

Figure S9. (A) Overlaid ^{1}H-^{15}N HSQC spectra of apo (red) and pCdc25C-bound Pin1$_{W34A/R17A}$ (blue). Cross-peaks of A140 and L141 that are sensitive probes for interdomain contact are zoomed for clarity. No chemical shift perturbation for either A140 or L141 was found between the two spectra, indicating that pCdc25C binding does not change the extent of interdomain contact of Pin1$_{W34A/R17A}$. (B) Overlaid ^{1}H-^{15}N HSQC spectra of pCdc25C-bound Pin1$_{W34A/R17A}$, Pin1$_{W34A}$ and Pin1$_{\Delta SG}$. The cross-peaks of A140 and L141 are zoomed for clarity. (C) The isomerization rates of Pin1$_{W34A/R17A}$ and Pin1$_{\Delta SG}$ for pCdc25C determined using ^{1}H-^{1}H EXSY experiments. (D) The isomerization rates of Pin1$_{W34A/R17A}$ and Pin1$_{\Delta NSSSG/W34A/R17A}$ for pCdc25C were determined using ^{1}H-^{1}H EXSY experiments. Pin1$_{\Delta NSSSG/W34A/R17A}$ exhibited a k_{EXSY} value (k_{ct} + k_{tc}) of 74.8 s^{-1}, approximately 3.6-fold higher than Pin1$_{W34A/R17A}$ that exhibited a k_{EXSY} value of 20.7 s^{-1}.

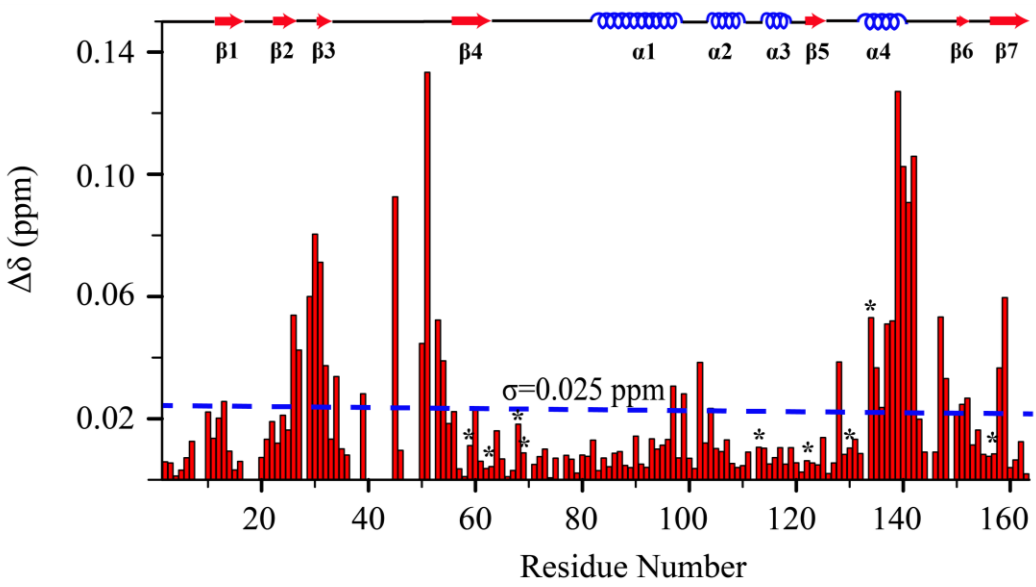

Figure S10. Chemical shift perturbations (Δδ) between wild-type Pin1 and Pin1$_{\Delta NSSSG}$. The Δδ values were calculated based on the ^{1}H-^{15}N HSQC spectra of Pin1 and Pin1$_{\Delta NSSSG}$. The resulted Δδ values were plotted versus residue number, the catalytic residues were labeled by asterisks. The residues with Δδ values larger than standard deviation (σ) were considered to be with significant chemical shift perturbations. Secondary structural elements of Pin1 were shown on top.

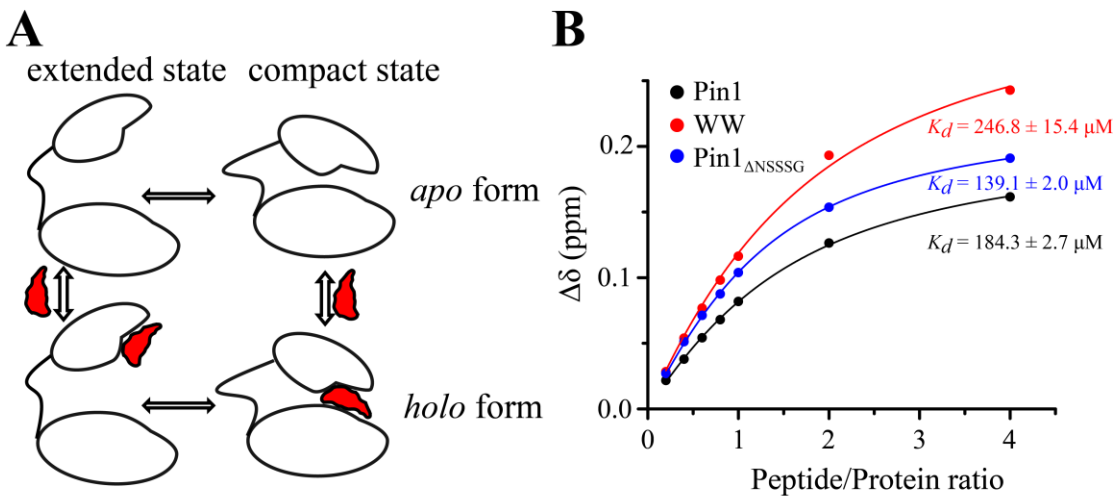

Figure S11. (A) The schematic diagram for thermodynamic cycle of substrate binding. Pin1 samples both compact and extended conformation in solution. Substrate binding shifts the dynamic equilibrium of the two states due to binding preference. (B) NMR titration curves for W34 of Pin1 (black curve), the isolated WW domain (red curve), and $Pin1_{\Delta NSSSG}$ (blue curve) with FFpSPR. The chemical shift perturbations (Δδ) were calculated using equation (2). To determine K_d values, Δδ values for a group of residues were globally fitted to equation (5), and only the fitting of Δδ from W34 is shown for illustration.